Microstructure and Properties of Cped Thermal Protective Coating Modified by Platinum Particles on Al-SI Alloy

Ping Wang (wangping0922@sina.com)
Xi'an Technological University
Xiaomin Chen
Xi'an Electronic Engineering Research Institute
Chunqing Zhang
Chengde Petroleum College
Di Jiao
Xi'an Technological University
Shangyi Jiao
Xi'an Technological University
Min Yao
Xi'an Technological University

Research Article

Keywords: Al-12Si alloy, Cathodeplasma electrolytic deposition (CPED), Heat insulation performance, Fracture toughness, Particle toughened coating

Posted Date: June 10th, 2020

DOI: https://doi.org/10.21203/rs.3.rs-34100/v1

Microstructure and properties of CPED thermal protective coating modified by platinum particles on Al-Si alloy

Ping Wang[1], Xiaomin Chen[2], Chunqing Zhang[3], Di Jiao[1], Shangyi Jiao[1], Min Yao[1]*

(1. School of Materials and Chemical Engineering, Xi'an Technological University, Xi'an 710021, China; 2. Xi'an Electronic Engineering Research Institute, Xi'an 710100, China; 3. Department of Mechanical Engineering, Chengde Petroleum College, Chengde 067000, China)

* Corresponding author: Tel.: +8613891910659; fax: +86 29 83208080. E-mail address:wping0922@163.com.

Abstract

The thermal protection layer of cathode plasma electrolytic deposition on platinum particles was prepared on Al-Si alloy. The microstructure and the heat insulation performance, fracture toughness and bending strength of the coating were investigated by SEM, XRD, the heat insulation test device and tensile testing machine. The distribution of platinum particles in the ceramic layer is uniform, which can effectively fill the micropores of plasma discharge. The ceramic layer is mainly composed of α-Al_2O_3 and t-ZrO_2, and there is the formation of high temperature stable phase $Zr_3Y_4O_{12}$ in the ceramic layer. With the increase of platinum particles, the heat insulation temperature, fracture toughness and bending strength gradually increase. After thermal shock, no obvious cracks were found on the surface of the coating, which indicated that the coating had good thermal shock resistance.

Keywords: Al-12Si alloy; Cathode plasma electrolytic deposition (CPED); Heat insulation performance; Fracture toughness; Particle toughened coating

1. Introduction

Cathode plasma electrolytic deposition (CPED) is a novel surface treatment

technology, which is not limited by the substrate metal and has good adhesion [1-5]. The ceramic coating has good wear resistance and corrosion resistance [6-8]. However, there are few reports on the CPED ceramic layer [9]. In particular, there are fewer reports on the mechanical properties of CPED ceramic layers [10-13]. Generally, the brittleness of the ceramic layer limits its mechanical properties such as fracture toughness. Therefore, the mechanical properties of the ceramic layer can be improved by phase transformation and toughening of particles, whiskers or fibers [14-18]. Zhong et al. [19] prepared $Gd_2Zr_2O_7$ coating by thermal spraying, which indicated that the ceramic layer was toughened by addition of nanostructured Y_2O_3 partially-stabilized ZrO_2 (3YSZ) to improve fracture toughness and the thermal shock performance of the matrix.

Metal ductile particles such as gold, silver and platinum can effectively toughen ceramic layer. Ma et al. [20] prepared Au nano-particles doped α-Al_2O_3 composite coating on TiAl-based alloy. It indicates that cracks were shielded by means of crack bridging and the fracture resistance can be improved by toughening effects of the composite structure. Pt is an ideal material for particle toughening due to its good oxidation resistance and ductility [21]. Deng et al. [22] prepared $La_2Zr_2O_7$ thermal barrier coatings (TBCs) with dispersed Pt particles by cathode plasma electrolytic deposition (CPED), which indicated that the ceramic coating had a good thermal insulation, high-temperature oxidation resistance and good mechanical properties because of the toughening effect of Pt particles. Wang et al. [23] prepared the porous α-Al_2O_3 thermal barrier coatings (TBCs) containing dispersed Pt particles by

cathode plasma electrolytic deposition (CPED). It indicates the coating provides good thermal insulation and exhibit excellent mechanical properties because of the toughening effect of the Pt particles and because of stress relaxation induced by deformation of the porous structure. Al-Si alloys as hot end components, such as pistons, withstand high temperatures and pressures. Therefore, the ceramic layer needs to have good heat resistance and mechanical properties. However, there are few studies on the thermal protection and mechanical properties of CPED coating on Al-Si alloy.

In the present study, $H_2PtCl_6 \cdot 6H_2O$ was chosen as an additive, and the effect of $H_2PtCl_6 \cdot 6H_2O$ on the microstructure and heat-insulating and mechanical properties of CPED coating on a cast Al-12Si alloy were investigated in detail.

2. Experimental

Al-12Si-3Cu-2Ni-1Mg (wt.%) alloy was used in the experiment. CPED ceramic layer was prepared by plasma electrolytic deposition equipment. Firstly, in order to induce cathode plasma discharge before CPED, PEO method was used to prepare insulating barrier layer. Al_2O_3 barrier layer with a thickness of 3 um was prepared for 2min in silicate solution. The current density was 5 A/dm^2 and duty cycle was 10%. During the CPED process, the specimen was used as cathode. After 30 minutes of treatment, the current density was 8 A/dm^2 and duty cycle was 30% in the CPED process. The experimental solution was $Zr(NO_3)_4$ (12 g/l), $Y(NO_3)_3$ (1 g/l) and $H_2PtCl_6 \cdot 6H_2O$ with concentrations between 0.08 g/L and 0.24 g/L.

The microstructure and phase composition of the coatings were tested by SEM

and XRD. The thermal insulation and thermal shock performance were tested through thermal insulation and thermal shock test equipment. The fracture toughness and bending strength were tested by tensile testing machine.

3. Results and discussion

3.1. Effect of Pt on microstructure and phase composition of CPED coating

Fig. 1 shows the microstructure of CPED coatings with different Pt contents. From the diagram, after adding Pt particles, the number of micropores in plasma discharge decreases and Pt particles distribute uniformly in the coating. With the increase of H_2PtCl_6 content, the content of Pt particles increases and grows.

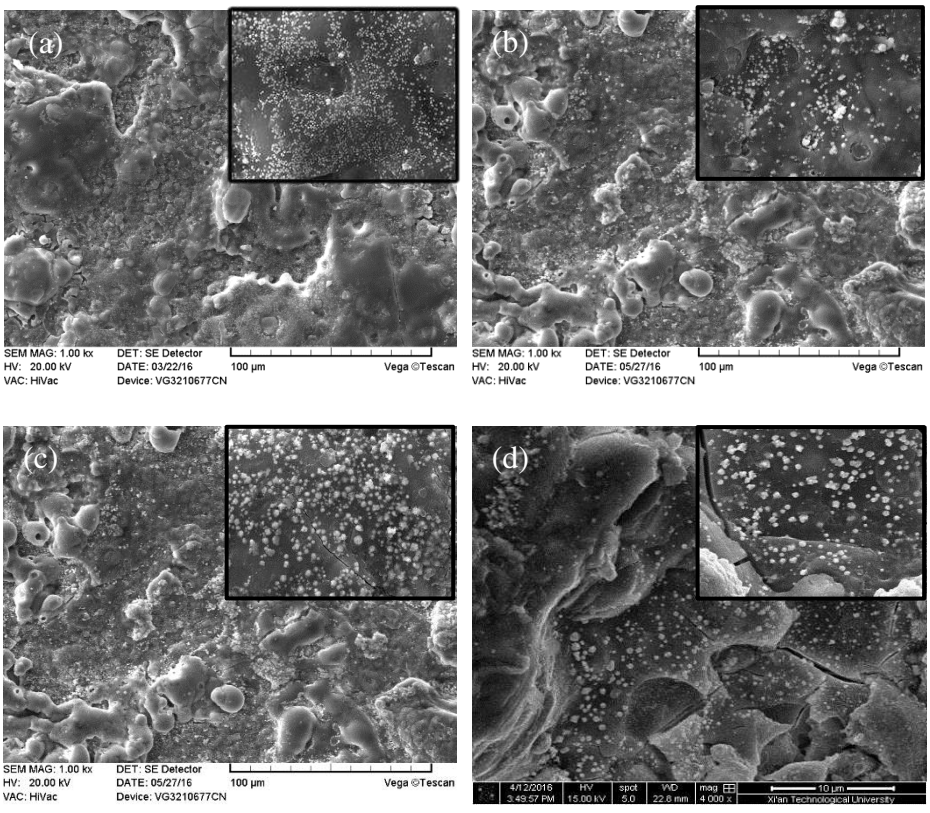

Fig. 1. Micromorphology of CPED coatings with different $H_2PtCl_6 \cdot 6H_2O$ concentrations: (a) 0.08 g/L; (b) 0.12 g/L; (c) 0.16 g/L; (d) 0.24 g/L

Fig. 2 is the XRD pattern of ceramic layer under different H_2PtCl_6 concentration. As seen in Fig. 2, the peak of Pt appeared at 40°, 46° and 68°. Moreover, with the increase of H_2PtCl_6 concentration, the characteristic peaks at 40° gradually increase. In addition, a high temperature solid solution phase $Zr_3Y_4O_{12}$ and a certain amount of α-Al_2O_3 and t-ZrO_2 were found in the ceramic layer. After adding Pt particles, high temperature phase $Zr_3Y_4O_{12}$ appeared in CPED ceramic coating. Due to the high conductivity of Pt, it is easy to produce cathodic plasma electrodeposition reaction, which makes the energy utilization rate of plasma electrolysis deposition reaction high. Therefore, the reaction temperature in the discharge channel is high, and it is easy to form high temperature phase $Zr_3Y_4O_{12}$. Fig.3 is the calculation result of the temperature field inside and outside the plasma discharge channel. It can be found that the temperature in the plasma discharge channel can reach 5723 ℃.

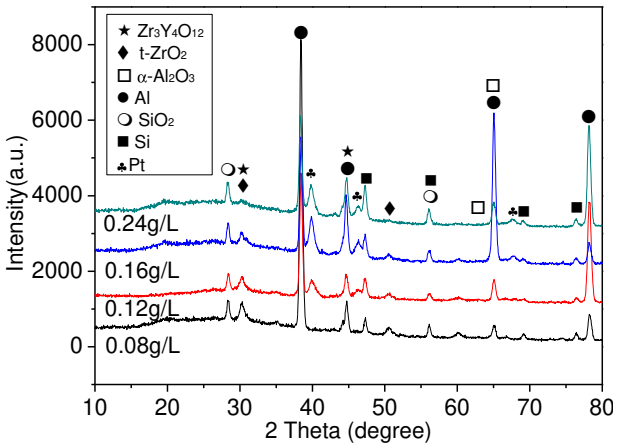

Fig. 2. XRD spectra of ceramic coatings at different $H_2PtCl_6 \cdot 6H_2O$ concentrations

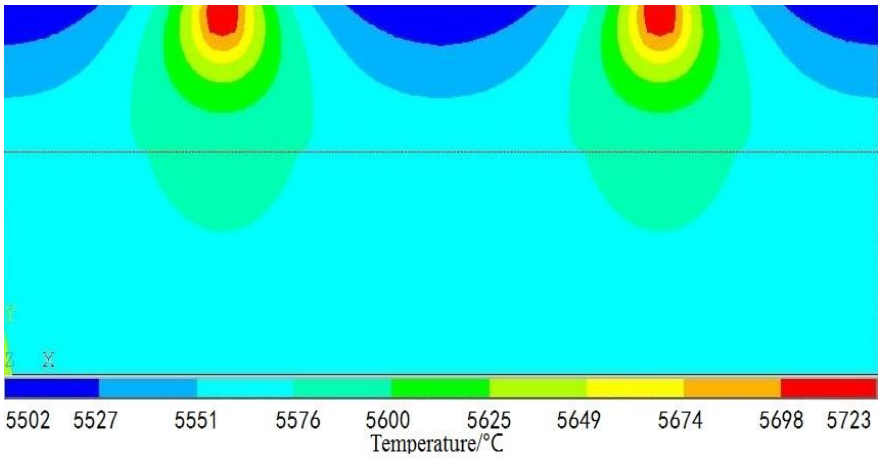

Fig. 3. Temperature field distribution of plasma discharge channel

3.2. Formation mechanism of coating modified by platinum particles

Fig.4 is the film forming mechanism model of Pt particle modified ceramic layer. With the increase of voltage, a large amount of H_2 is produced on the cathode (chemical reaction formula(1)), which is wrapped on the surface of the cathode to form a gas barrier film(Fig.4a). At the same time, the electrolysis of water generates OH^- in the cathode area. With the increase of voltage, the strong electric field between cathode and anode will break through the barrier film in the weak area of cathode surface and the surrounding hydrogen film, and the plasma micro arc discharge will occur. At first, the number of plasma micro arc discharge is small, and then with the reaction, the number of plasma discharge gradually increases(Fig.4b).

In the process of cathodic plasma electrooxidation, the sample is used as cathode. Al^{3+}, Zr^{4+}, Y^{3+} and Pt^{4+} in the electrolyte move towards the cathode surface under the strong electric field, and then the hydroxide layer is formed by the reaction of Al^{3+}, Zr^{4+}, Y^{3+} with OH^- in solution(chemical reaction formula(2),(3),(4)). With the increase of voltage, a large amount of heat is generated, and the temperature in the discharge

channel rises sharply. The hydroxide dehydrates under high temperature and forms the molten oxide. Under the action of strong electric field, the oxide ejected along the discharge channel solidifies rapidly to form oxide ceramics after encountering cold electrolyte(chemical reaction formula(5),(6),(7)). In this process, Pt^{4+} in the electrolyte also enters the film along the discharge channel. Under the action of the instantaneous high temperature generated by the micro arc discharge, the electrons of platinum ions on the cathode surface are reduced(reaction formula(10)), ejected along the discharge channel, and condensed and sintered rapidly to form composite ceramic coating. Finally, the molten oxide deposits in the channel mouth to form a crater like shape, and accumulates in island shape around it, or blocks in the discharge channel. The gas phase that did not erupt in time forms a hole in the channel, while the Pt particles are evenly deposited in the ceramic layer(Fig.4c).

$$2H_2O+2e\rightarrow 2OH^-+H_2 \quad (1)$$

$$Zr^{4+}+4OH^-\rightarrow Zr(OH)_4 \quad (2)$$

$$Y^{3+}+3OH^-\rightarrow Y(OH)_3 \quad (3)$$

$$Al^{3+}+3OH^-\rightarrow Al(OH)_3 \quad (4)$$

$$Zr(OH)_4\rightarrow ZrO_2+2H_2O \quad (5)$$

$$2Y(OH)_3\rightarrow Y_2O_3+3H_2O \quad (6)$$

$$2Al(OH)_3\rightarrow Al_2O_3+3H_2O \quad (7)$$

$$Si^{4+}+2O^{2-}\rightarrow SiO_2 \quad (8)$$

$$3Zr^{4+}+4Y^{3+}+24OH^-\rightarrow Zr_3Y_4O_{12}+12H_2O \quad (9)$$

$$Pt^{4+}+4e^-\rightarrow Pt \quad (10)$$

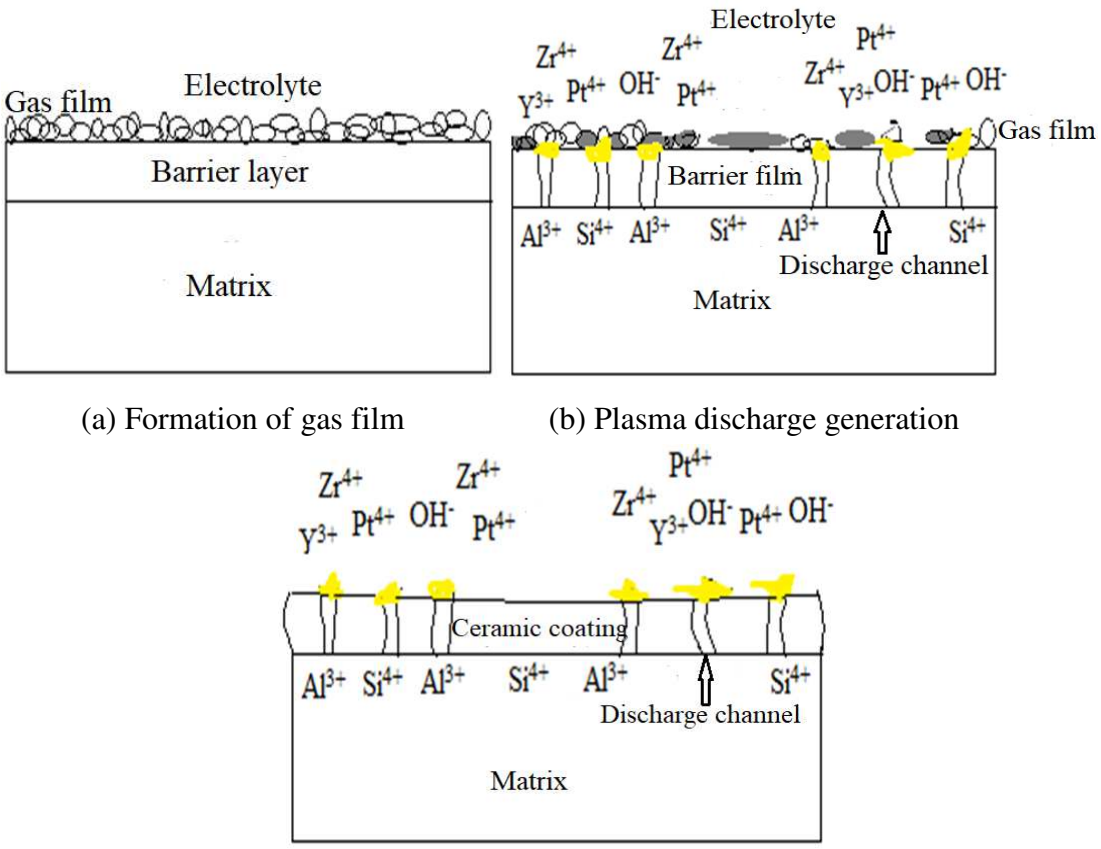

(a) Formation of gas film (b) Plasma discharge generation

(c) Ceramic layer formation

Fig. 4. Film forming mechanism model of Pt particle modified ceramic layer

3.3. Heat insulation performance of CPED coating

Fig.5 shows the thermal insulation temperature curve of CPED coating under the action of platinum particles. As seen in Fig.5, with the increase of the concentration of $H_2PtCl_6 \cdot 6H_2O$, the insulation temperature increases gradually. Thermal insulation performance is related to thermal conductivity and microstructure of ceramic coating. The thermal conductivity of Al_2O_3 in ceramic coating is 30W/(m·k), while that of ZrO_2 is 2 W/(m·k). Because Pt particles promote the plasma electrolysis reaction, more high temperature stable phases t-ZrO_2 are formed, so the heat insulation performance is improved. On the other hand, Pt particles can effectively fill the micropores of plasma discharge and increase the number of closed pores on the

coating surface. The sealed micropores reduce the thermal conductivity and improve the thermal insulation performance of the coating.

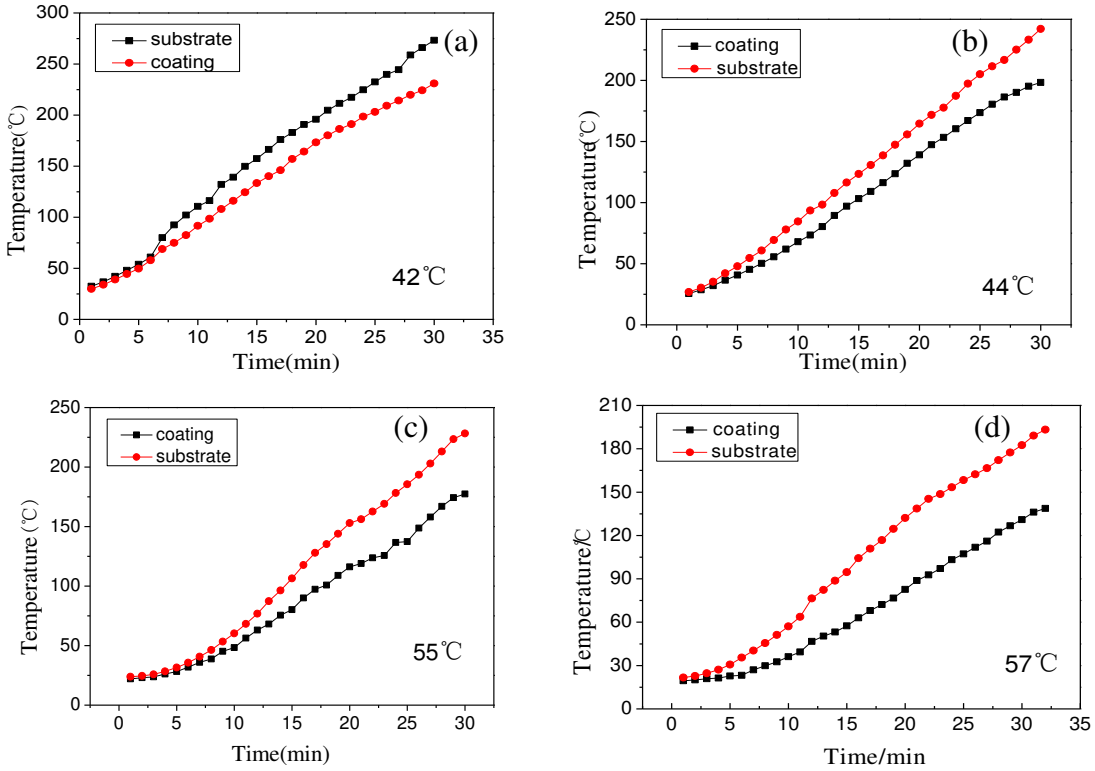

Fig.5. Heat-insulating temperature test of CPED coatings for different $H_2PtCl_6 \cdot 6H_2O$ concentrations: (a) 0.08 g/L; (b) 0.12 g/L; (c) 0.16 g/L and (d) 0.24 g/L.

3.4. Thermal shock performance of CPED coating

The surface morphology of the ceramic coating with 500 thermal shock tests at 450 ℃ is shown in Fig.6. As seen in Fig.6, after the thermal shock test of the ceramic layer before and after the addition of $H_2PtCl_6 \cdot 6H_2O$, the macro morphology of the sample surface did not change significantly, and the coating did not show cracks or peeling off. From the micro morphology after thermal shock, without the addition of Pt particles, there are obvious microcracks on the surface of the ceramic layer. After adding Pt particles, the microcracks are not obvious. Because ductile Pt particles can absorb crack energy, passivate crack, reduce crack growth rate and improve thermal shock

performance.

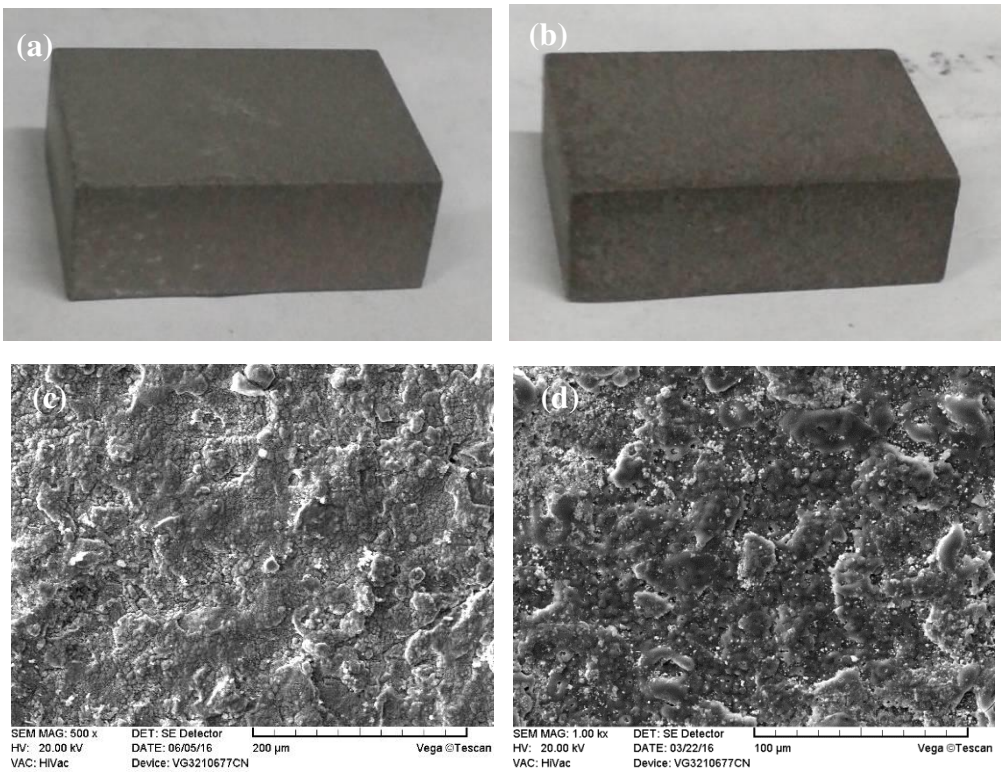

Fig.6. Macroscopic and microscopic morphology after thermal shock

(a), (c) 0 g/L $H_2PtCl_6 \cdot 6H_2O$; (b), (d) 0.16 g/L $H_2PtCl_6 \cdot 6H_2O$

3.5. Fracture toughness and bending strength of coatings with Pt particles addition

Fig.7 shows the effect of chloroplatinic acid on fracture toughness and bending strength of coatings. As seen in Fig.7, the fracture toughness and bending strength of the coatings increased with the addition of chloroplatinic acid. Moreover, with the increase of chloroplatinic acid concentration, the fracture toughness and bending strength increased gradually.

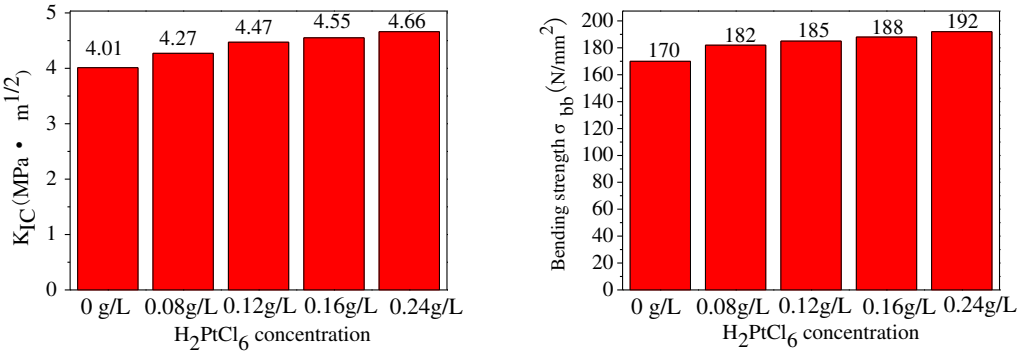

(a) Fracture toughness (b) Bending strength

Fig.7. Fracture toughness and bending strength of coatings

3.6. Mechanism of CPED ceramic coating toughened by platinum particles

When the thermal protective coating works at high temperature, the change of temperature will cause thermal stress in the coating. When the thermal stress exceeds the critical fracture stress, the crack will propagate unsteadily and the coating will fail and peel off. The criteria of brittle ceramic coating cracking and peeling are as follows:

$$\frac{(1-\nu)\sigma_{coating}^{2}h}{E_{coating}} > G_c \quad (11)$$

$E_{coating}$ is the elastic modulus of the coating, ν is the Poisson's ratio of the coating, h is the thickness of the coating, $\sigma_{coating}$ is the thermal stress of the coating, and Gc is the fracture toughness in the form of energy. When the coating material meets the formula, the peeling failure of the coating can be avoided. It can be seen that there are two ways to avoid coating peeling failure when the thickness of the coating is fixed. One is to reduce the driving force of crack initiation and propagation, that is, to reduce $\sigma_{coating}$; the other is to improve the fracture toughness Gc of the coating by means of toughening.

Because the content of Pt particles deposited in the coating is small, it has little effect on the phase transition sintering and thermal expansion coefficient of the coating, so it is difficult to reduce the thermal stress in the coating by slowing down the phase change sintering of the coating or increasing the thermal expansion coefficient of the coating. Therefore, the failure of the coating can be avoided by toughening the ceramic coating and improving the fracture toughness of the coating.

Pt particles toughen ceramic coating mainly through bridging and crack deflection. Fig.8(a) and Fig.9(a) is the schematic diagram of crack bridging toughening mechanism. When the crack propagates to Pt particles, Pt particles can absorb the energy of crack propagation through plastic deformation and prevent further crack propagation. Fig.8(b) and Fig.9(b) is the schematic diagram of crack deflection toughening mechanism.

In the process of crack growth, the crack will propagate along the grain boundary around Pt particles. The crack interlock phenomenon will appear, so the friction bridge will be formed, which will consume the energy of crack growth and avoid further crack growth. In addition, due to the Pt particles in the ceramic coating and the formation characteristics of the ceramic coating, a large number of microcracks will form in front of the ceramic coating when the crack propagates. Microcracks improve the fracture toughness of ceramic coatings by absorbing the energy of lattice strain and relieving the stress concentration at the crack tip. Therefore, the ductile Pt particles can improve the fracture toughness of the coating.

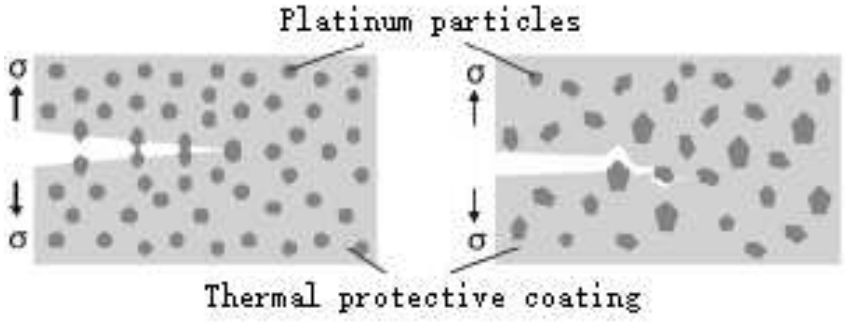

(a) Bridge toughening mechanism (b) Mechanism of crack deflection toughening

Fig.8 Toughening mechanism model of Pt particles

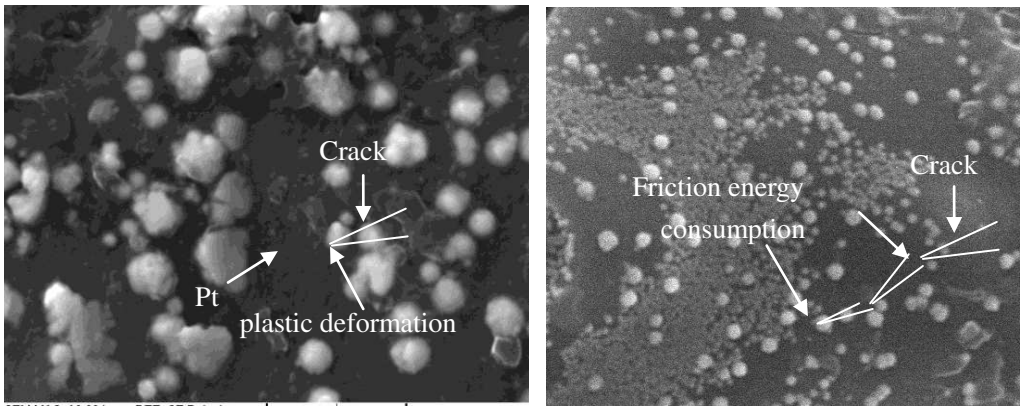

(a) Bridging toughening of Pt particles (b) Crack deflection toughening of Pt particles

Fig.9 Toughening mechanism of Pt particles

In addition, according to Griffith fracture theory, fracture toughness can be expressed by formula (12). K_{IC} is the fracture toughness expressed by the stress field intensity factor, σ_c is the critical crack growth stress, a is the half length of the crack.

$$K_{IC}=\sigma_c \sqrt{a} \cdot \tag{12}$$

The more Pt particles are dispersed in a unit volume of ceramic coating, the greater the resistance of crack to Pt particles in the process of propagation, and the smaller the average size of crack. Therefore, the toughening effect of ceramic coating will be improved, and the fracture toughness will be better. In addition, Rice's research on the toughening mechanism of particle doping shows that if there are too

many toughening particles in the coating, the particles may agglomerate. At this time, the toughening effect of continuing to increase the number of particles on the coating will be very limited.

4. Conclusions

The microstructure, thermal insulation and fracture toughness of CPED ceramic coating modified by platinum particles were studied. It can be seen from the calculation that the temperature in the cathode plasma discharge channel can reach 5723 ℃. The distribution of platinum particles in the ceramic layer is uniform, which can effectively fill the micropores of plasma discharge, and the evenly closed micropores can effectively improve the thermal insulation performance of the ceramic layer. The ceramic layer is mainly composed of α-Al_2O_3 and t-ZrO_2, and there is the formation of high temperature stable phase $Zr_3Y_4O_{12}$ in the ceramic layer. The reduction deposition of Pt^{4+} ions on the cathode surface can effectively improve the thermal insulation, fracture toughness and bending strength of the ceramic coating. After thermal shock, no obvious cracks were found on the surface of the coating, which indicated that the coating had good thermal shock resistance. Pt particles can improve the mechanical properties of the ceramic layer through the mechanism of bridge toughening and crack deflection toughening.

Acknowledgment

This research work is financially supported by the Youth Innovation Team of Shaanxi Universities: Metal corrosion protection and surface engineering technology, the National Natural Science Foundation of China (51771140), Industrial field project

of Shaanxi provincial science and technology department (2018GY-111), Shaanxi provincial department of education industrialization cultivation project (17JF009) and Yulin science and technology project (2018-2-30).

Conflict of Interest

The authors declare that they have no conflict of interest.

References

[1] M.H. Li, D.R. Wang, J.C. Xue, R.X. Jia, Direct preparation of $Y_3Al_5O_{12}$ hollow microspheres using cathode plasma electrolytic deposition, Ceramics International, 45(2019)24919-24922.

[2] P. Wang, Q.Q. Yuwen, J.P, Li, The differences in the formation mechanism of PEO and CPED composited ceramic coatings on Al-12Si alloy, Journal of Alloys and Compounds, 788 (2019) 61-66.

[3] J.C. Xue, D.R Wang, M.H. Li, R.X. Jia, Preparation of silicon-modified gamma alumina coating through cathodic plasma electrolytic deposition, Ceramics International, 45(2019)19345-19350.

[4] C. Quan, S.J. Deng, Y.D. Jiang, C. Jiang, M.B. Shuai, Characteristics and high temperature oxidation behavior of Ni-Cr-Y_2O_3 nanocomposite coating prepared by cathode plasma electrolytic deposition, Journal of Alloys and Compounds, 793(2019)170-178.

[5] P. Wang, J.P, Li, Z.J. Ma, P.H. Gao, The growth mechanism of CPED coating with zirconia sol addition on an Al-12Si alloy. Journal of Alloys and compounds, 740(2018)735-742.

[6] R.N. Ji, G.C. Peng, S.G. Zhang, Z. Li, J.S. Wu, The fabrication of a CeO_2 coating via cathode plasma electrolytic deposition for the corrosion resistance of AZ31 magnesium alloy, Ceramics International, 44(2018)19885-19891.

[7] J.W. Huang, J.Y. Zhu, X.M. Fan, D.S. Xiong, J.L. Li, Preparation of MoS_2-Ti(C, N)-TiO_2 coating by cathodic plasma electrolytic deposition and its tribological properties, Surface and Coatings Technology, 347(2018)76-83.

[8] Y. Wang, X.Q. Cao, Z. Zhang, K. Huang, J.S Wu, Formation and wear performance of diamond-like carbon films on 316L stainless steel prepared by cathodic plasma electrolytic deposition, Diamond and Related Materials, 95(2019)135-140.

[9] S.Q. Wang, F.Q. Xie, X.Q. Wu, Mechanism of Al_2O_3 coating by cathodic plasma electrolytic deposition on TiAl alloy in $Al(NO_3)_3$ ethanol-water electrolytes, Materials Chemistry and Physics, 202(2017)114-119.

[10] S.G. Zhang, J. Zhang, R.N. Ji, Y. Lian, Y.D. He, The effect of electric conductivity on the structure of ceramic coatings prepared by cathode plasma electrolytic deposition, Materials Chemistry and Physics, 224(2019)36-39.

[11] L.Z. Ma, J.W. Huang, X.M. Fan, J.L. Li, D.S. Xiong, Properties of thick ceramic composite coatings synthesized on an aluminium alloy by cathodic plasma electrolytic deposition, Surface and Coatings Technology, 356(2018)80-88.

[12] L.X. Wang, D.R. Wang, Study on energy consumption of Al_2O_3 coating prepared by cathode plasma electrolytic deposition, Ceramics International, 44 (2018)657-662.

[13] P. Wang, S.J. Deng, Y.D. He, C.X. Liu, J. Zhang, Oxidation and hot corrosion behavior of Al_2O_3/YSZ coatings prepared by cathode plasma electrolytic deposition, Corrosion Science, 109(2016) 13-21.

[14] R.X. Shi, J. Li, Y.S. Yin, H.Y. Ge, Toughening mechanisms and microstructure of Al_2O_3-TiC-Co composites, Materials Science and Engineering: A, 528(2011) 5341-5347.

[15] S.J. Deng, P. Wang, Y.D. He, J. Zhang, Thermal barrier coatings with Al_2O_3-Pt composite bond-coat and $La_2Zr_2O_7$-Pt top-coat prepared by cathode plasma electrolytic deposition, Surface and Coatings Technology, 291(2016) 141-150.

[16] M.H. Li, D.R. Wang, J.C. Xue, R.X. Jia, Preparation of Pd-doped $Y_3Al_5O_{12}$ thermal barrier coatings using cathode plasma electrolytic deposition, Ceramics International, 46(2020)7019-7024.

[17] C.X. Liu, S.G. Zhang, R.N. Ji, P. Wang, Y.D. He, Cathode plasma electrolytic deposition of Al_2O_3 coatings doped with SiC particles, Ceramics International, 45(2019)4747-4755.

[18] S.Q. Wang, F.Q. Xie, X.Q. Wu, L.Y. Chen, CeO_2 doped Al_2O_3 composite ceramic coatings fabricated on γ–TiAl alloys via cathodic plasma electrolytic deposition, Journal of Alloys and Compounds, 788(2019)632-638.

[19] X.H. Zhong, H.Y. Zhao, X.M. Zhou, C.G. Liu, L. Wang, Thermal shock behavior of toughened gadolinium zirconate/YSZ double-ceramic-layered thermal barrier coating, Journal of Alloys and Compounds, 593(2014)50-55.

[20] X.X. Ma, Y.D. He, D.R. Wang, Preparation and high-temperature properties of Au nano-particles doped alpha-Al_2O_3 composite coating on TiAl-based alloy, Applied Surface Science, 257(2011) 10273-10281.

[21] S.J. Deng, C. Jiang, T.W. Liu, M.B. Shuai, P. Wang, Characteristics of Al_2O_3-Pt/YSZ-Pt double layer composite coatings prepared by cathode plasma electrolytic deposition, Rare Metal Materials and Engineering, 47 (2018)3590-3596.

[22] S.J. Deng, P. Wang, Y.D. He, J. Zhang, $La_2Zr_2O_7$ TBCs toughened by Pt particles prepared by cathode plasma electrolytic deposition, International Journal of Minerals, Metallurgy, and Materials, 23(2016) 704-715.

[23] P. Wang, Y.D. He, S.J. Deng, J. Zhang, Porous α-Al_2O_3 thermal barrier coatings with dispersed Pt particles prepared by cathode plasma electrolytic deposition, International Journal of Minerals, Metallurgy, and Materials, 23(2016)92-101.

Figures

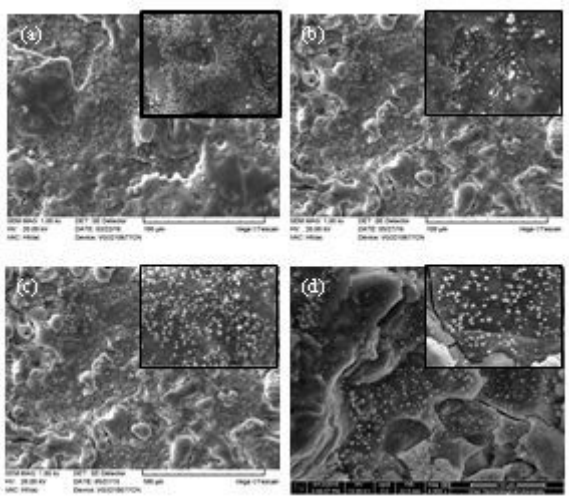

Figure 1

Micromorphology of CPED coatings with different H2PtCl6•6H2O concentrations: (a) 0.08 g/L; (b) 0.12 g/L; (c) 0.16 g/L; (d) 0.24 g/L

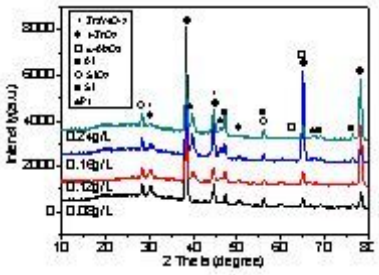

Figure 2

XRD spectra of ceramic coatings at different H2PtCl6•6H2O concentrations

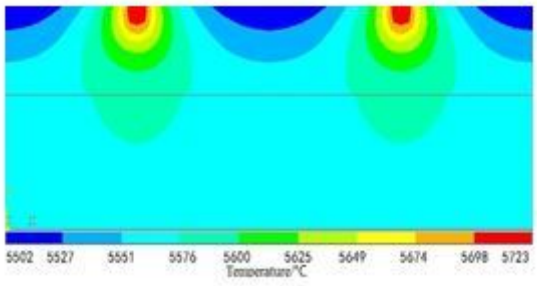

Figure 3

Temperature field distribution of plasma discharge channel

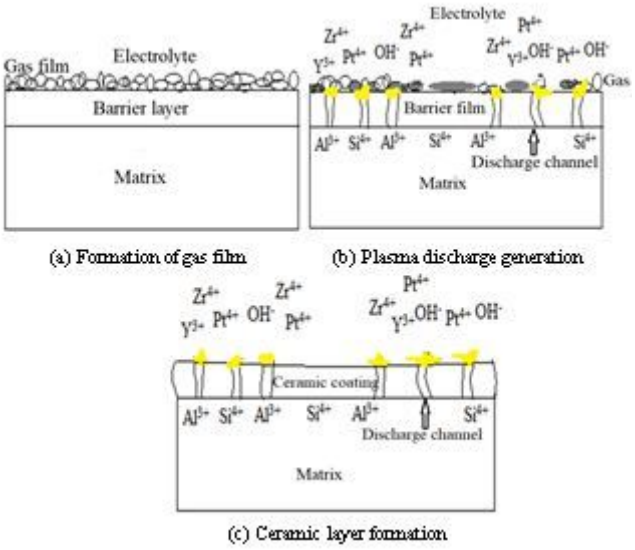

Figure 4

Film forming mechanism model of Pt particle modified ceramic layer

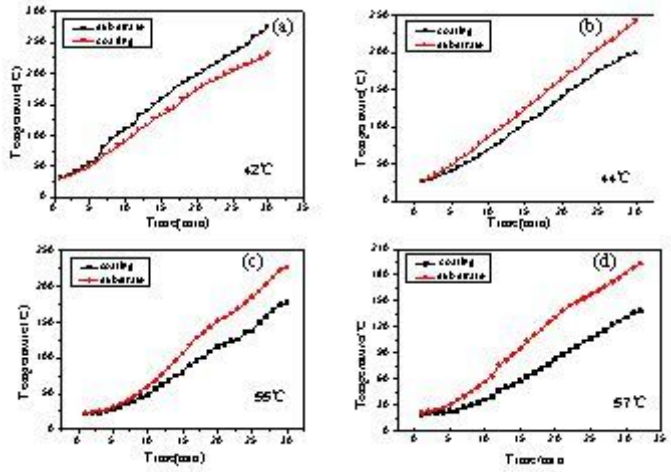

Figure 5

Heat-insulating temperature test of CPED coatings for different H2PtCl6•6H2O concentrations: (a) 0.08 g/L; (b) 0.12 g/L; (c) 0.16 g/L and (d) 0.24 g/L.

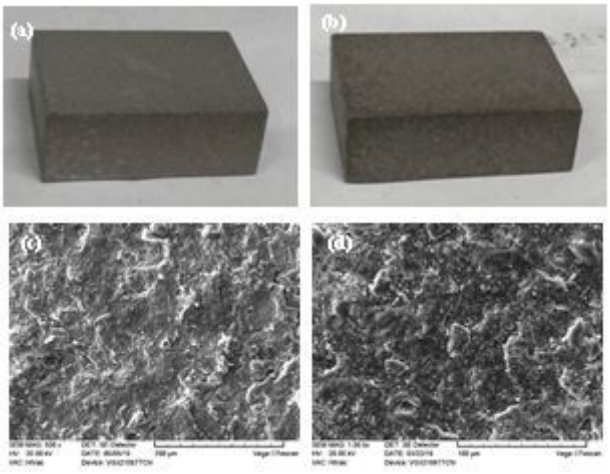

Figure 6

Macroscopic and microscopic morphology after thermal shock (a), (c) 0 g/L H2PtCl6•6H2O; (b), (d) 0.16 g/L H2PtCl6•6H2O

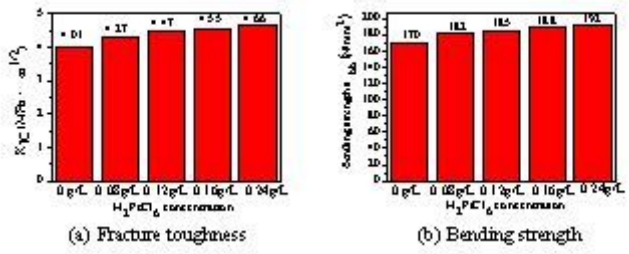

Figure 7

Fracture toughness and bending strength of coatings

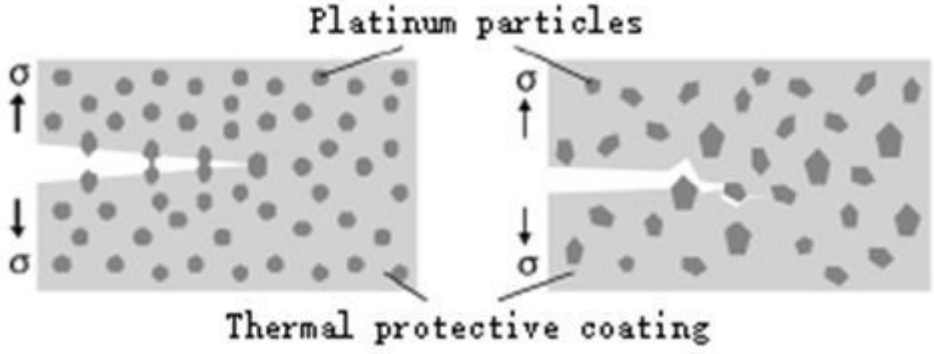

Figure 8

Toughening mechanism model of Pt particles

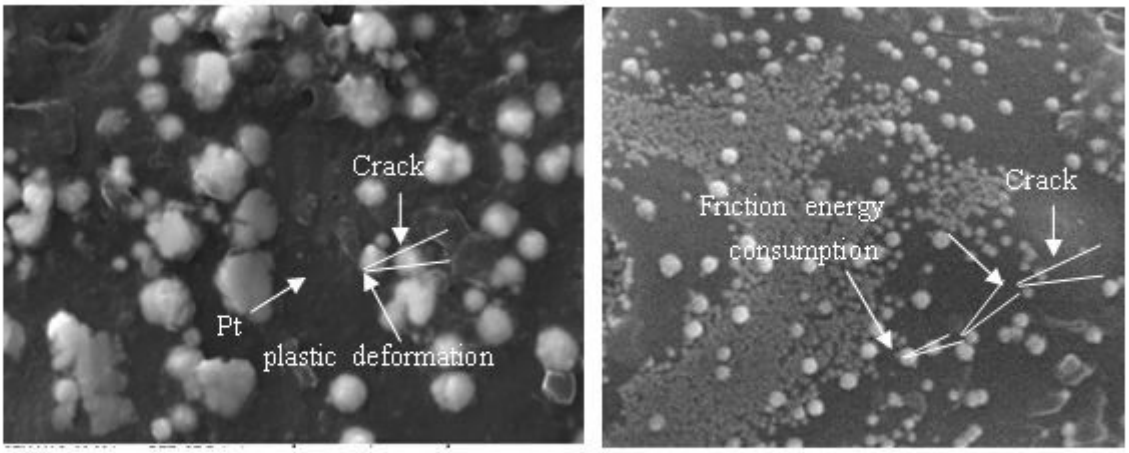

(a) Bridging toughening of Pt particles (b) Crack deflection toughening of Pt particles

Figure 9

Toughening mechanism of Pt particles